Bull. Natl. Mus. Nat. Sci., Ser. C, 42, pp. 5–17, December 22, 2016

Reference samples to learn calcareous nannofossil biostratigraphy from Miocene to Pleistocene

Kyoko Hagino[1], Masayuki Utsunomiya[2], Yuichiro Tanaka[2] and Masao Iwai[1]

[1] Center for Advanced Marine Core Research, Kochi University,
200 Monobe-otsu, Nankoku, Kochi 780–8502, Japan
[2] Research Institute of Geology and Geoinformation, Geological Survey of Japan, AIST,
Tsukuba, Ibaraki 305–8567, Japan

Abstract Reference smear slides of Miocene–Pleistocene calcareous nannofossils were prepared for educational purposes, using deep-sea core sediments collected from the Indian Ocean during Ocean Drilling Program (ODP) Leg 115. Light microscopic images of calcareous nannofossil index taxa found from the reference samples are shown, and the characteristics of calcareous nannofossil assemblages from the Miocene to Pleistocene are introduced briefly.

Key words: biostratigraphy, calcareous nannofossils, Miocene, Pliocene, Pleistocene

Introduction

Calcareous nannofossils have a continuous fossil record from the Triassic through the Pleistocene, and are widely used for dating marine sediments. The classification of calcareous nannofossils is primary based on morphology, size, and crystallographic characteristics (e.g. Bown, 1998). The orientation of the crystallographic axis of the calcite elements forming calcareous nannofossils is stable within lineages, and so is used for family/genus level classification. Some calcareous nannofossil lineages are relatively stable in morphology, but have greatly changed in size of fossils across their evolutionary histories. They produced remarkably large fossils in some specific age-intervals. Those large specimens are useful for dating sediments, and are occasionally separated from common-sized specimens as 'index species'. Identification of those large 'index species' is often problematic, since many calcareous nannofossil lineages have experienced size-enlargement events multiple times in their evolutionary histories, and the large 'index species' from a specific geological age are often confusingly similar in appearance to the other large 'index species' from different geological ages. For the utilization of such large 'index species' for biostratigraphy, it is essential to understand co-occurring taxa that can narrow down the possible age of the sediments. Therefore, not only understanding of definition of index species but also characteristics/composition of total nannofossil assemblages in geological ages are required for the dating of marine sediments based on calcareous nannofossils.

In order to help beginner researchers to learn calcareous nannofossil biostratigraphy, we have launched a project to prepare and provide reference samples from Triassic through Pleistocene. We plan to prepare samples for this project using the samples, which have already been studied by experienced researchers, since the information of fossil assemblages revealed by experienced researchers are useful for understanding of classification of fossils for beginners. As the first step of this project, we have prepared four sets of reference smear slides from Miocene to Pleistocene sediments collected and studied by Ocean Drilling Program (ODP) Leg 115 participants (Okada, 1990; Rio *et al.*, 1990; Shipboard Scientific Party, 1988). In this paper, we introduce our reference slides with the light microscopic images of index species found from these slide sets, and briefly introduce change in calcareous nannofossil assemblages in the Neogene and the Quaternary.

Materials and Methods

A total of 142 samples were collected from the Miocene–Pleistocene Sections 709C-1H-1 through -22X-1 of ODP Leg 115 at approximately 1.5 m intervals. Four sets of smear slides were prepared from each sample, and were stored in the National Museum of Nature and Science and in the Kochi Core Center (Kochi University) (Table 1). Smear slide samples were examined under a polarized light microscope (Nikon E600 POL), and representative individual of the index species as well as its co-occuring taxa were photographed by a CCD camera (Nikon DS L3) (Figs. 1–10). Focus stacking images were produced for some taxa with steric structure using a software (Nikon NIS-Elements D).

Introduction to Miocene-Pleistocene Calcareous Nannofossil Biostratigraphy

Table 1 lists the sediments used for preparation of reference slides, and calcareous nannofossil zone and age of each smear slide assigned by previous studies (Okada, 1990; Rio *et al.*, 1990; Shipboard Scientific Party, 1988). Figures 1–5 show major index fossil species observed from our reference samples, and figures 6–10 are the examples of appearance of calcareous nannofossil assemblages in the lower and upper Miocene, lower and upper Pliocene, and Pleistocene.

Typical calcareous nannofossils can be observed under cross-polarized light microscope. However, fossils produced by some lineages are invisible or dark/obscure under cross-polarized light for their crystallographic orientation. Therefore, observations of the samples that may contain the taxa invisible/obscure under the cross-polarized light should be made in both cross- and plane- polarized light. In the Cenozoic calcareous nannofossils, the lineages with dark/obscure liths under cross-polarized light, such as *Discoaster* spp. and *Amaurolithus* spp., occur from the sediments 1.95 Ma or older (Raffi *et al.*, 2006; Young, 1997). Therefore, the samples likely to be 1.95 Ma or older should be examined using both cross- and plane- polarized light, while the samples certainly younger than 1.95 Ma can be examined only by cross-polarized light.

Early Miocene to early Pliocene calcareous nannofossil assemblages older than 3.6 Ma (NN1-15 in Martini, 1981; CN1-11 in Okada and Bukry, 1980) are characterized by diversification of *Sphenolithus* spp. and *Discoaster* spp. (Figs. 1–4) and change in size of placolith-bearing lineages. Members of *Sphenolithus* are particularly useful for dating early Miocene sediments (Figs. 1h–lk), on the other hand, the *Discoaster* species are useful for dating middle Miocene to early Pliocene sediments (Figs. 2, 3). In this period, *Coccolithus* and *Reticulofenestra* coccoliths changed in size greatly, and their large fossils are used as 'index species' in biostratigraphy together with the other index species. *Coccolithus* produced remarkably large ($>14\,\mu$m) specimens called *Coccolithus eopelagicus* ($>14\,\mu$m) (Figs. 1e, 6a) and *Coccolithus miopelagicus* ($>14\,\mu$m) (Figs. 1f, 7a) from the Eocene-very early Miocene and in the middle Miocene, respectively. *C. eopelagicus* coexists with common *Cyclicargolithus floridanus* (Figs. 1b, 6a) and *Sphenolithus* species with early-Miocene forms (Figs. 1h–1k), while *C. miopelagicus* co-occurs with small-medium sized *Reticulofenestra* species (Fig. 7) (e.g. Young *et al.*, 1998). *Reticulofenestra pseudoumbilicus*, which is identified by their large size ($>7\,\mu$m), appeared in two separated time intervals in middle Miocene (Fig. 1a) and in the early Pliocene (Figs. 4h, 8) (e.g. Young, 1998). They disappeared tentatively in the middle Miocene in the zone NN10 (Backman *et al.*, 2012) or at around CN 8a/8b (Okada and Bukry, 1980) boundary. They recurred in the late Miocene, while disappeared again at the NN15/NN16 (Martini, 1971) or CN 11b/CN12a (Okada and Bukry, 1980) boundaries.

Late Pliocene to very early Pleistocene calcar-

Table 1. Samples used for preparation of smear slide, depth of the source sediment, calcareous nannofossil zones and age of the samples assigned by previous studies. Fossil zones for the samples the samples from 1H-1, 2.0–3.0 cm through 4H-6, 20.0–21.0 cm referred Shipboard Scientific Party (1988)[1], and the samples from 4H-7, 10.0–11.0 cm through 21X-1 43.0–44.0 cm referred Rio *et al.* (1988)[2].

Source sediment of slide samples	Depth of samples below the sea floor (mbsf)	Biozone by Okada and Bukry (1980)	Biozone by Martini (1971)	Age of sediments	Reference
Hole 709C-1H-1, 2.0–3.0 cm	0.02	CN15	NN21	Pleistocene	1
Hole 709C-1H-2, 12.0–13.0 cm	1.62	CN15	NN21	Pleistocene	1
Hole 709C-1H-3, 2.0–3.0 cm	3.02	CN14b	NN20	Pleistocene	1
Hole 709C-1H-4, 12.0–13.0 cm	4.62	CN14b	NN20	Pleistocene	1
Hole 709C-2H-1, 2.0–3.0 cm	5.82	CN14a	NN19	Pleistocene	1
Hole 709C-2H-2, 12.0–13.0 cm	7.42	CN14a	NN19	Pleistocene	1
Hole 709C-2H-3, 2.0–3.0 cm	8.82	CN14a	NN19	Pleistocene	1
Hole 709C-2H-4, 12.0–13.0 cm	10.42	CN14a	NN19	Pleistocene	1
Hole 709C-2H-5, 2.0–3.0 cm	11.82	CN14a	NN19	Pleistocene	1
Hole 709C-2H-6, 10.0–11.0 cm	13.40	CN14a	NN19	Pleistocene	1
Hole 709C-2H-7, 5.0–6.0 cm	14.85	CN14a	NN19	Pleistocene	1
Hole 709C-3H-1, 5.0–6.0 cm	15.45	CN14a	NN19	Pleistocene	1
Hole 709C-3H-2, 10.0–11.0 cm	17.00	CN13	NN19	Upper Pliocene	1
Hole 709C-3H-3, 5.0–6.0 cm	18.45	CN12c	NN17–18	Upper Pliocene	1
Hole 709C-3H-4, 10.0–11.0 cm	20.00	CN12c	NN17–18	Upper Pliocene	1
Hole 709C-3H-5, 5.0–6.0 cm	21.45	CN12c	NN17–18	Upper Pliocene	1
Hole 709C-3H-6, 10.0–11.0 cm	23.00	CN12c	NN17–18	Upper Pliocene	1
Hole 709C-3H-7, 5.0–6.0 cm	24.45	CN12b	NN17–18	Upper Pliocene	1
Hole 709C-4H-1, 10.0–11.0 cm	25.20	CN12b	NN16	Upper Pliocene	1
Hole 709C-4H-2, 20.0–21.0 cm	26.80	CN12b	NN16	Upper Pliocene	1
Hole 709C-4H-3, 10.0–11.0 cm	28.20	CN12a	NN16	Upper Pliocene	1
Hole 709C-4H-4, 5.0–6.0 cm	29.65	CN12a	NN16	Upper Pliocene	1
Hole 709C-4H-5, 10.0–11.0 cm	31.20	CN12a	NN16	Upper Pliocene	1
Hole 709C-4H-6, 20.0–21.0 cm	32.80	CN12a	NN16	Upper Pliocene	1
Hole 709C-4H-7, 10.0–11.0 cm	34.20	CN12a	NN16	Upper Pliocene	2
Hole 709C-5H-1, 10.0–11.0 cm	34.80	CN12a	NN16	Lower Pliocene	2
Hole 709C-5H-2, 5.0–6.0 cm	36.25	CN11	NN15	Lower Pliocene	2
Hole 709C-5H-3, 10.0–11.0 cm	37.80	CN11	NN15	Lower Pliocene	2
Hole 709C-5H-4, 5.0–6.0 cm	39.25	CN11	NN15	Lower Pliocene	2
Hole 709C-5H-5, 11.0–12.0 cm	40.81	CN11	NN15	Lower Pliocene	2
Hole 709C-5H-6, 5.0–6.0 cm	42.25	CN11	NN15	Lower Pliocene	2
Hole 709C-5H-7, 10.0–11.0 cm	43.80	CN11	NN15	Lower Pliocene	2
Hole 709C-6H-1, 10.0–11.0 cm	44.40	CN11	NN15	Lower Pliocene	2
Hole 709C-6H-2, 5.0–6.0 cm	45.85	CN10c	NN13 − NN14	Lower Pliocene	2
Hole 709C-6H-3, 15.0–16.0 cm	47.45	CN10c	NN13 − NN14	Lower Pliocene	2
Hole 709C-6H-4, 5.0–6.0 cm	48.85	CN10c	NN13 − NN14	Lower Pliocene	2
Hole 709C-6H-5, 14.0–15.0 cm	50.44	CN10c	NN13 − NN14	Lower Pliocene	2
Hole 709C-6H-6, 4.0–5.0 cm	51.84	CN10c	NN13 − NN14	Lower Pliocene	2
Hole 709C-6H-7, 14.0–15.0 cm	53.44	CN10b	NN12	Lower Pliocene	2
Hole 709C-7H-1, 14.0–15.0 cm	54.04	CN10b	NN12	Lower Pliocene	2
Hole 709C-7H-2, 4.0–5.0 cm	55.44	CN10b	NN12	Lower Pliocene	2
Hole 709C-7H-3, 14.0–15.0 cm	57.04	CN10b	NN12	Lower Pliocene	2
Hole 709C-7H-4, 4.0–5.0 cm	58.44	CN10a	NN12	Lower Pliocene	2
Hole 709C-7H-5, 14.0–15.0 cm	60.04	CN10a	NN12	Lower Pliocene	2
Hole 709C-7H-6, 4.0–5.0 cm	61.44	CN9b	NN11	Upper Miocene	2
Hole 709C-8H-1, 89.0–90.0 cm	64.49	CN9b	NN11	Upper Miocene	2
Hole 709C-8H-2, 43.0–44.0 cm	65.53	CN9b	NN11	Upper Miocene	2
Hole 709C-8H-3, 43.0–44.0 cm	67.03	CN9b	NN11	Upper Miocene	2
Hole 709C-8H-4, 43.0–44.0 cm	68.53	CN9b	NN11	Upper Miocene	2
Hole 709C-8H-5, 43.0–44.0 cm	70.03	CN9b	NN11	Upper Miocene	2
Hole 709C-8H-6, 43.0–44.0 cm	71.53	CN9b	NN11	Upper Miocene	2
Hole 709C-8H-7, 43.0–44.0 cm	73.03	CN9b	NN11	Upper Miocene	2
Hole 709C-9H-1, 43.0–44.0 cm	73.63	CN9b	NN11	Upper Miocene	2
Hole 709C-9H-2, 43.0–44.0 cm	75.13	CN9b	NN11	Upper Miocene	2
Hole 709C-9H-3, 43.0–44.0 cm	76.63	CN9b	NN11	Upper Miocene	2
Hole 709C-9H-4, 43.0–44.0 cm	78.13	CN9b	NN11	Upper Miocene	2
Hole 709C-9H-5, 43.0–44.0 cm	79.63	CN9b	NN11	Upper Miocene	2
Hole 709C-9H-6, 41.0–42.0 cm	81.11	CN9b	NN11	Upper Miocene	2
Hole 709C-9H-7, 22.0–23.0 cm	82.42	CN9b	NN11	Upper Miocene	2
Hole 709C-10H-1, 47.0–48.0 cm	83.37	CN9b	NN11	Upper Miocene	2
Hole 709C-10H-2, 43.0–44.0 cm	84.83	CN9b	NN11	Upper Miocene	2
Hole 709C-10H-3, 43.0–44.0 cm	86.33	CN9b	NN11	Upper Miocene	2
Hole 709C-10H-4, 43.0–44.0 cm	87.83	CN9b	NN11	Upper Miocene	2
Hole 709C-10H-5, 43.0–44.0 cm	89.33	CN9b	NN11	Upper Miocene	2
Hole 709C-10H-6, 43.0–44.0 cm	90.83	CN9a	NN11	Upper Miocene	2
Hole 709C-10H-7, 43.0–44.0 cm	92.33	CN9a	NN11	Upper Miocene	2
Hole 709C-11H-1, 43.0–44.0 cm	92.93	CN9a	NN11	Upper Miocene	2
Hole 709C-11H-2, 43.0–44.0 cm	94.43	CN9a	NN11	Upper Miocene	2
Hole 709C-11H-3, 43.0–44.0 cm	95.93	CN9a	NN11	Upper Miocene	2
Hole 709C-11H-4, 43.0–44.0 cm	97.43	CN9a	NN11	Upper Miocene	2
Hole 709C-11H-5, 43.0–44.0 cm	98.93	CN9a	NN11	Upper Miocene	2

Table 1. Continued.

Source sediment of slide samples	Depth of samples below the sea floor (mbsf)	Biozone by Okada and Bukry (1980)	Biozone by Martini (1971)	Age of sediments	Reference
Hole 709C-12H-1, 57.0–58.0 cm	102.77	CN9a	NN11	Upper Miocene	2
Hole 709C-12H-2, 43.0–44.0 cm	104.13	CN9a	NN11	Upper Miocene	2
Hole 709C-12H-3, 43.0–44.0 cm	105.63	CN9a	NN11	Upper Miocene	2
Hole 709C-12H-4, 43.0–44.0 cm	107.13	CN8	NN10	Upper Miocene	2
Hole 709C-12H-5, 43.0–44.0 cm	108.63	CN8	NN10	Upper Miocene	2
Hole 709C-12H-6, 43.0–44.0 cm	110.13	CN8	NN10	Upper Miocene	2
Hole 709C-12H-7, 43.0–44.0 cm	111.63	CN8	NN10	Upper Miocene	2
Hole 709C-13H-1, 43.0–44.0 cm	112.23	CN8	NN10	Upper Miocene	2
Hole 709C-13H-2, 43.0–44.0 cm	113.73	CN7	NN9	Upper Miocene	2
Hole 709C-13H-3, 43.0–44.0 cm	115.23	CN6	NN8	Upper Miocene	2
Hole 709C-13H-4, 43.0–44.0 cm	116.73	CN5b	NN7	Middle Miocene	2
Hole 709C-13H-5, 43.0–44.0 cm	118.23	CN5b	NN7	Middle Miocene	2
Hole 709C-13H-6, 43.0–44.0 cm	119.73	CN5b	NN7	Middle Miocene	2
Hole 709C-13H-7, 43.0–44.0 cm	121.23	CN5b	NN7	Middle Miocene	2
Hole 709C-14H-1, 43.0–44.0 cm	121.83	CN5a	NN6	Middle Miocene	2
Hole 709C-14H-2, 43.0–44.0 cm	123.33	CN5a	NN6	Middle Miocene	2
Hole 709C-14H-3, 43.0–44.0 cm	124.83	CN5a	NN6	Middle Miocene	2
Hole 709C-14H-4, 43.0–44.0 cm	126.33	CN5a	NN6	Middle Miocene	2
Hole 709C-14H-5, 43.0–44.0 cm	127.83	CN4	NN5	Middle Miocene	2
Hole 709C-14H-6, 43.0–44.0 cm	129.33	CN4	NN5	Middle Miocene	2
Hole 709C-14H-7, 43.0–44.0 cm	130.83	CN4	NN5	Middle Miocene	2
Hole 709C-15H-1, 43.0–44.0 cm	131.53	CN4	NN5	Middle Miocene	2
Hole 709C-15H-2, 43.0–44.0 cm	133.03	CN4	NN5	Middle Miocene	2
Hole 709C-15H-3, 43.0–44.0 cm	134.53	CN4	NN5	Middle Miocene	2
Hole 709C-15H-4, 43.0–44.0 cm	136.03	CN4	NN5	Middle Miocene	2
Hole 709C-15H-5, 43.0–44.0 cm	137.53	CN4	NN5	Middle Miocene	2
Hole 709C-15H-6, 43.0–44.0 cm	139.03	CN4	NN5	Middle Miocene	2
Hole 709C-15H-7, 43.0–44.0 cm	140.53	CN4	NN5	Middle Miocene	2
Hole 709C-16H-1, 43.0–44.0 cm	141.23	CN3	NN4	Lower Miocene	2
Hole 709C-16H-2, 43.0–44.0 cm	142.73	CN3	NN4	Lower Miocene	2
Hole 709C-16H-3, 43.0–44.0 cm	144.23	CN3	NN4	Lower Miocene	2
Hole 709C-16H-4, 43.0–44.0 cm	145.73	CN3	NN4	Lower Miocene	2
Hole 709C-16H-5, 56.0–57.0 cm	147.36	CN3	NN4	Lower Miocene	2
Hole 709C-16H-6, 43.0–44.0 cm	148.73	CN3	NN4	Lower Miocene	2
Hole 709C-16H-7, 40.0–41.0 cm	150.20	CN3	NN4	Lower Miocene	2
Hole 709C-17H-1, 43.0–44.0 cm	150.93	CN3	NN4	Lower Miocene	2
Hole 709C-17H-2, 43.0–44.0 cm	152.43	CN3	NN4	Lower Miocene	2
Hole 709C-17H-3, 43.0–44.0 cm	153.93	CN3	NN4	Lower Miocene	2
Hole 709C-17H-4, 43.0–44.0 cm	155.43	CN3	NN4	Lower Miocene	2
Hole 709C-17H-5, 43.0–44.0 cm	156.93	CN3	NN4	Lower Miocene	2
Hole 709C-17H-6, 43.0–44.0 cm	158.43	CN3	NN4	Lower Miocene	2
Hole 709C-17H-7, 43.0–44.0 cm	159.93	CN3	NN4	Lower Miocene	2
Hole 709C-18H-1, 43.0–44.0 cm	160.63	CN3	NN4	Lower Miocene	2
Hole 709C-18H-2, 43.0–44.0 cm	162.13	CN3	NN4	Lower Miocene	2
Hole 709C-18H-3, 43.0–44.0 cm	163.63	CN3	NN4	Lower Miocene	2
Hole 709C-18H-4, 43.0–44.0 cm	165.13	CN3	NN4	Lower Miocene	2
Hole 709C-18H-5, 43.0–44.0 cm	166.63	CN3	NN4	Lower Miocene	2
Hole 709C-18H-6, 43.0–44.0 cm	168.13	CN3	NN4	Lower Miocene	2
Hole 709C-18H-7, 43.0–44.0 cm	169.63	CN3	NN4	Lower Miocene	2
Hole 709C-19H-1, 43.0–44.0 cm	170.33	CN2	NN2	Lower Miocene	2
Hole 709C-19H-2, 43.0–44.0 cm	171.83	CN2	NN2	Lower Miocene	2
Hole 709C-19H-3, 43.0–44.0 cm	173.33	CN2	NN2	Lower Miocene	2
Hole 709C-19H-4, 43.0–44.0 cm	174.83	CN2	NN2	Lower Miocene	2
Hole 709C-19H-5, 43.0–44.0 cm	176.33	CN2	NN2	Lower Miocene	2
Hole 709C-19H-6, 43.0–44.0 cm	177.83	CN2	NN2	Lower Miocene	2
Hole 709C-19H-7, 43.0–44.0 cm	179.33	CN2	NN2	Lower Miocene	2
Hole 709C-20H-1, 43.0–44.0 cm	179.93	CN2	NN2	Lower Miocene	2
Hole 709C-20H-2, 43.0–44.0 cm	181.43	CN2	NN2	Lower Miocene	2
Hole 709C-20H-3, 43.0–44.0 cm	182.93	CN2	NN2	Lower Miocene	2
Hole 709C-20H-4, 43.0–44.0 cm	184.43	CN2	NN2	Lower Miocene	2
Hole 709C-20H-5, 43.0–44.0 cm	185.93	CN2	NN2	Lower Miocene	2
Hole 709C-20H-6, 43.0–44.0 cm	187.43	CN2	NN2	Lower Miocene	2
Hole 709C-20H-7, 43.0–44.0 cm	188.93	CN2	NN2	Lower Miocene	2
Hole 709C-21X-1, 43.0–44.0 cm	189.53	CN2	NN2	Lower Miocene	2
Hole 709C-21X-2, 43.0–44.0 cm	191.03	CN2	NN2	Lower Miocene	2
Hole 709C-21X-3, 43.0–44.0 cm	192.53	CN1a–CN1b	NN1	Lower Miocene	2
Hole 709C-21X-4, 43.0–44.0 cm	194.03	CN1a–CN1b	NN1	Lower Miocene	2
Hole 709C-21X-5, 43.0–44.0 cm	195.53	CN1a–CN1b	NN1	Lower Miocene	2
Hole 709C-21X-6, 43.0–44.0 cm	197.03	CN1a–CN1b	NN1	Lower Miocene	2
Hole 709C-22X-1, 43.0–44.0 cm	199.13	CN1a–CN1b	NN1	Lower Miocene	2

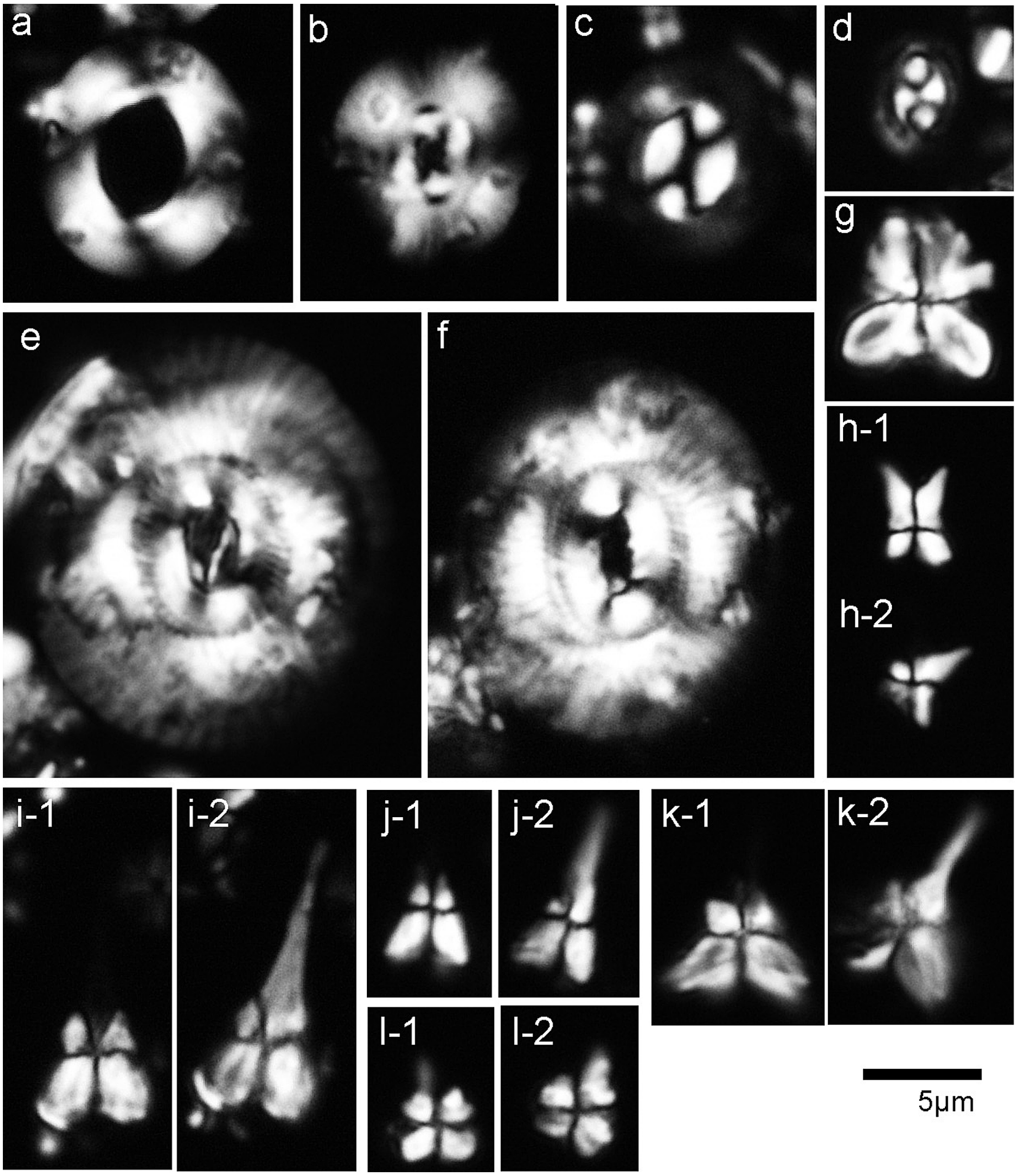

Fig. 1. Cross-polarized light microscopic images of calcareous nannofossil index fossil species from the Miocene. Note. Fossil zones assigned for each taxon follows Nannotax 3 (http://ina.tmsoc.org/Nannotax3/index.html). **a**, *Reticulofenestra pseudoumbilicus* (Sample 709C-13H-5, 44.0–45.0 cm) (NN4-NN15, CN3-CN11); **b**, *Cyclicargolithus floridanus* (Sample 709C-17H-7, 43.0–44.0 cm) (NP15-NN7, CP15-CN5a); **c**, *Coccolithus pelagicus* (Sample 709C-18H-3, 43.0–44.0 cm) (Paleocene–Present); **d**, *Hughesius tasmaniae* (Sample 709C-17H-7, 43.0–44.0 cm) (Oligocene- NN9, CN7); **e**, *Coccolithus eopelagicus* (Sample 709C-22X-1, 43.0–44.0 cm) (NP23-NN1, CP17-CN1); **f**, *Coccolithus miopelagicus* (Sample 709C-13H-5, 44.0–45.0 cm) (NN5-NN8, CN4-CN6); **g**, *Sphenolithus moriformis* (Sample 709C-17H-4, 43.0–44.0 cm) (Eocene- NN10, CN8); **h-1** and **h-2**, *Sphenolithus capricornutus* (Sample 709C-21X-5, 43.0–44.0 cm) (NP25-NN1, CP19-CN1); **i-1** and **i-2**, *Sphenolithus heteromorphus* (Sample 709C-17H-7, 43.0–44.0 cm) (NN4-NN5, CN3-CN4); **j-1** and **j-2**, *Sphenolithus belemnos* (Sample 709C-17H-7, 43.0–44.0 cm) (NN3, CN2); **k-1** and **k-2**, *Sphenolithus delphix* (Sample 709C-21X-5, 43.0–44.0 cm) (NP25-NN1, CP19a-CN1); **l-1** and **l-2**, *Sphenolithus conicus* (Sample 709C-17H-7, 43.0–44.0 cm) (NP25-NN3, CP19a-CN2).

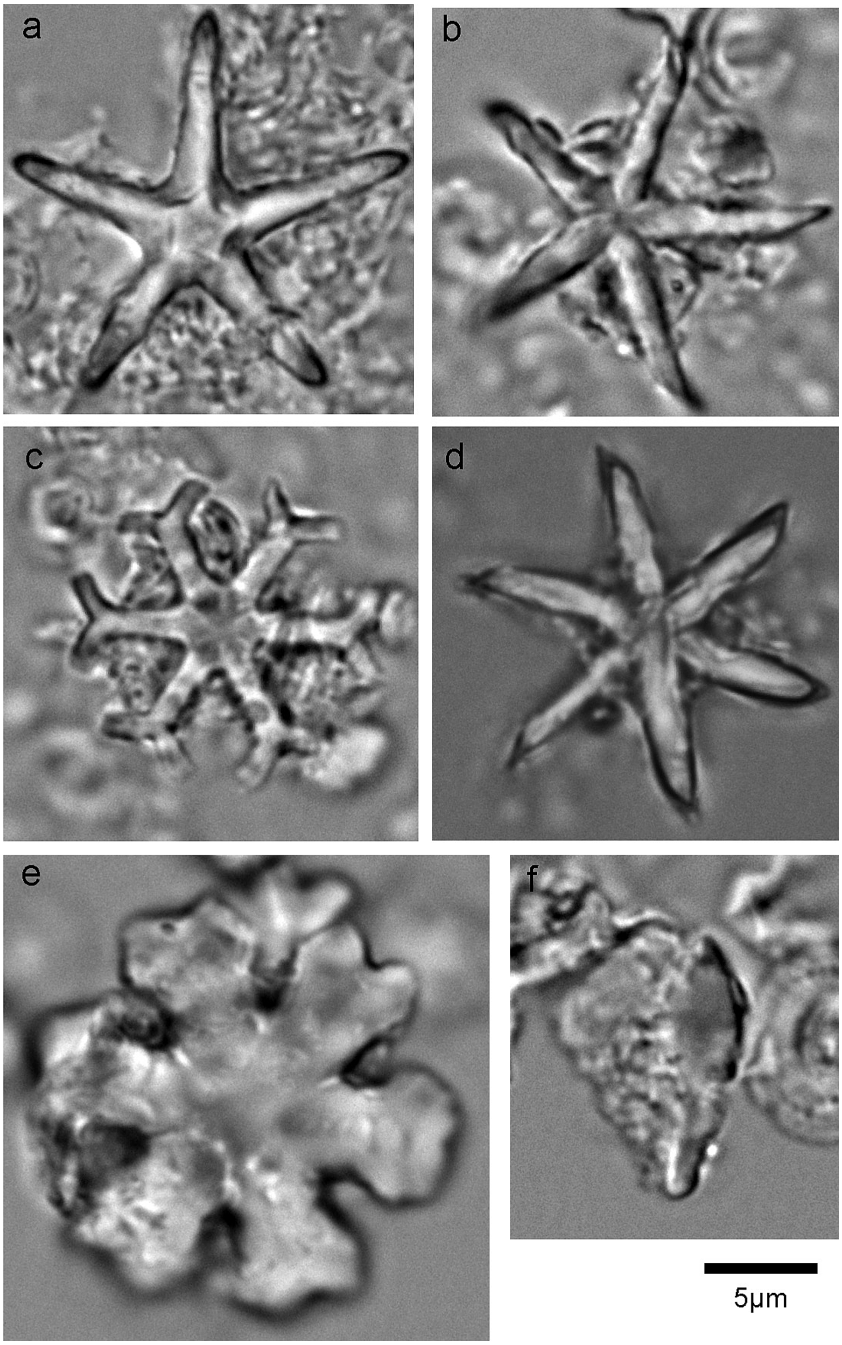

Fig. 2. Plane-polarized light microscopic images of calcareous nannofossil index fossil species from Miocene. Note. Fossil zones assigned for each taxon follows Nannotax 3 (http://ina.tmsoc.org/Nannotax3/index.html). **a**, *Discoaster quinqueramus* (Sample 709C-8H-6, 43.0–44.0 cm) (NN11, CN9); **b**, *Discoaster hamatus* (Sample 709C-12H-1, 57.0–58.0 cm) (NN9, CN7); **c**, *Discoaster challengeri* (Sample 709C-7H-8, 4.0–5.0 cm) (NN5-NN10, CN4-CN9); **d**, *Discoaster calcaris* (Sample 709C-12H-1, 57.0–58.0 cm) (NN9-NN11, CN7-CN9); **e**, *Discoaster druggii* (Hole 709C-19H-1, 43.0–44.0 cm) (NN2-NN3, CN1c-CN2); **f**, *Orthorhabdus*/*Triquetrorhabdulus rugosus* (Sample 709C-14H-1, 43.0–44.0 cm) (NN6-NN12, CN5a-CN10ab).

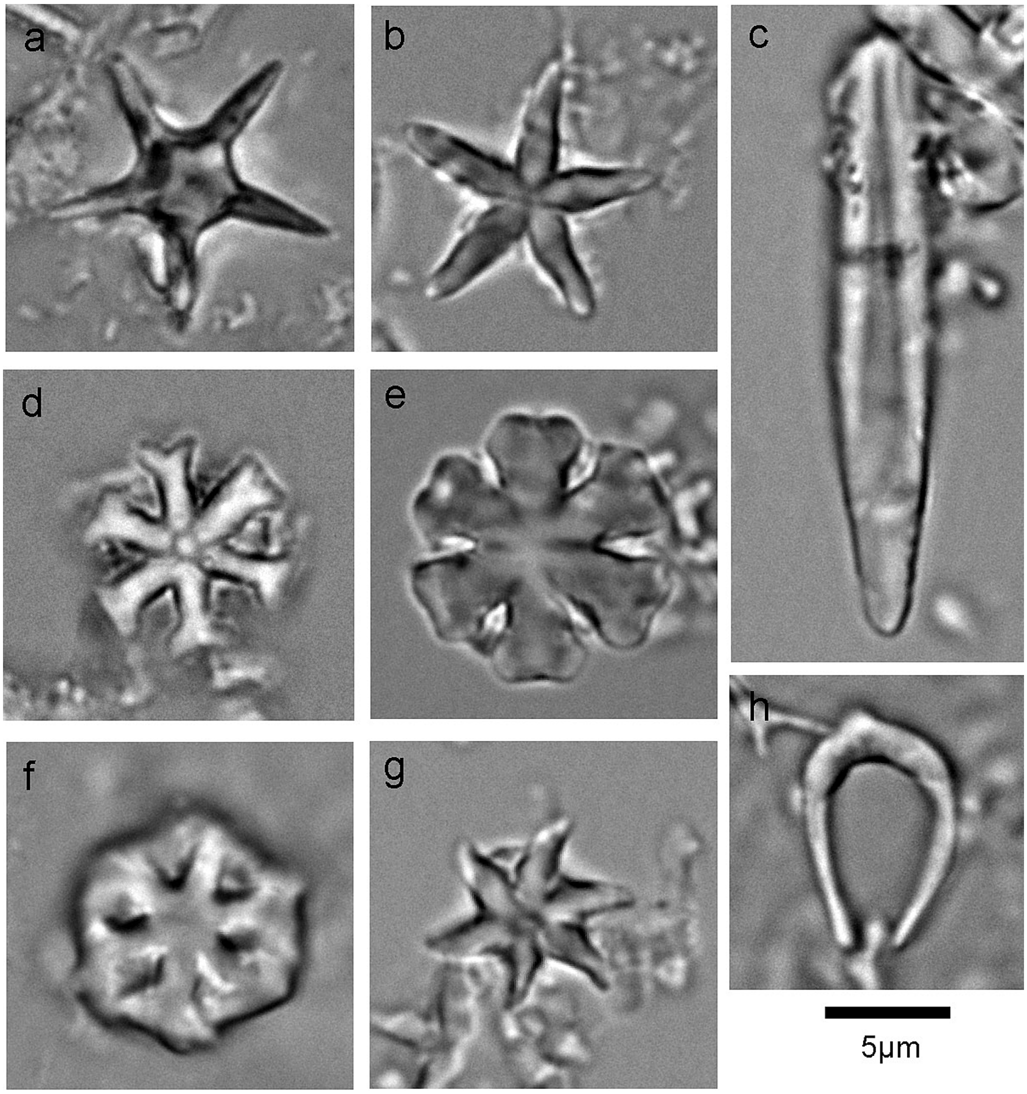

Fig. 3. Plane-polarized light microscopic images of calcareous nannofossil index fossil species from the Miocene. Note. Fossil zones assigned for each taxon follows Nannotax 3 (http://ina.tmsoc.org/Nannotax3/index.html). **a**, Focus stacking images of *Discoaster berggrenii* (Sample 709C-9H-2, 24.0–25.0 cm) (NN11a, CN9); **b**, *Discoaster bellus* (Sample 709C-12H-1, 57.0–58.0 cm) (NN8-NN11, CN6-CN9); **c**, *Triquetrorhabdulus carinatus* (Sample 709C-17H-7, 43.0–44.0 cm) (NP25-NN2, CP19a-CN1c); **d**, *Discoaster bollii* (Sample 709C-19H-1, 43.0–44.0 cm) (NN8-NN9, CN6- CN7); **e**, *Discoaster deflandrei* (Sample 709C-16H-1, 44.0–45.0 cm) (NP13-NN7, CP11-CN5b); **f**, *Catinaster coalitus* (Sample 709C-13H-2, 44.0–45.0 cm) (NN8-NN10, CN6-CN8); **g**, *Catinaster calyculus* (Sample 709C-13H-2, 44.0–45.0 cm) (NN9-NN10, CN7-CN8); **h**, *Amaurolithus* sp. (Sample 709C-9H-2, 24.0–25.0 cm) (NN11b-NN14, CN9b-CN10d).

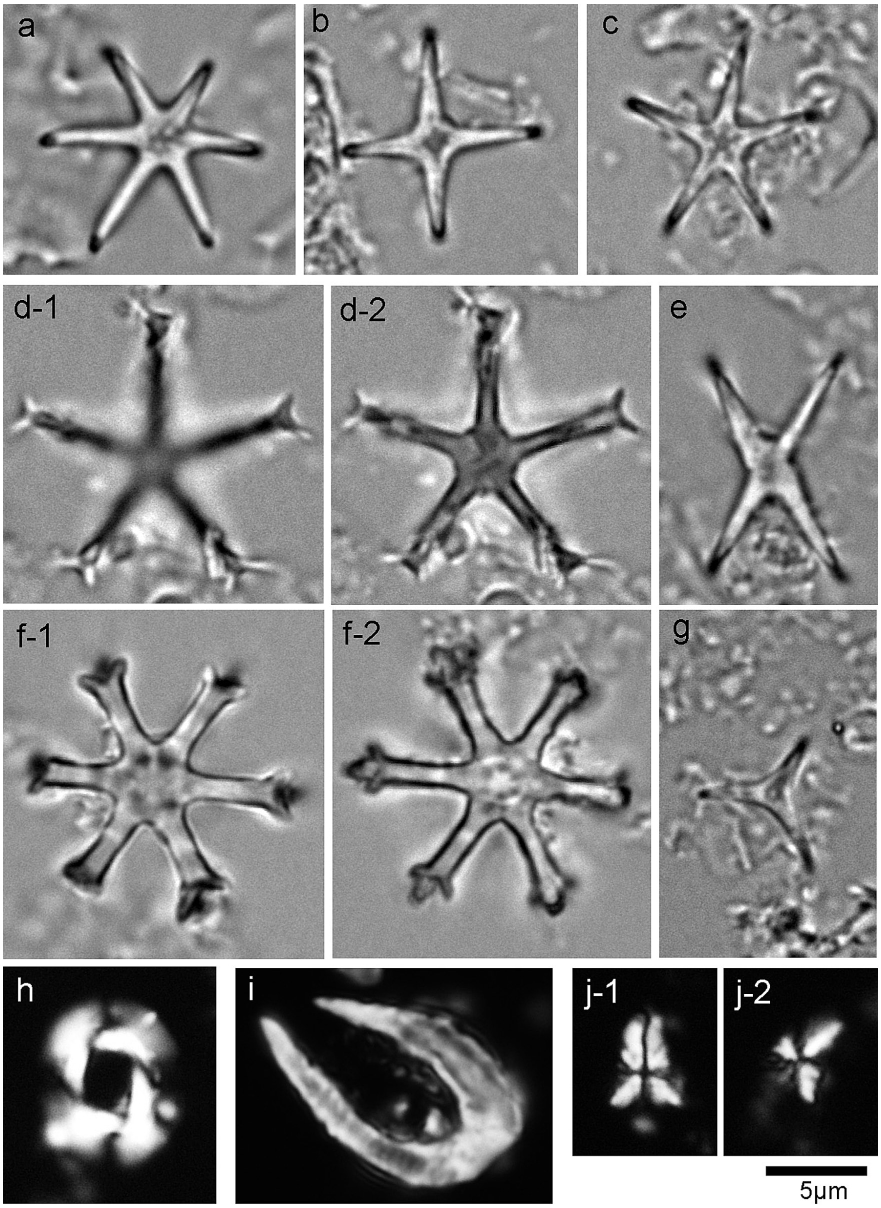

Fig. 4. Plane- or cross polarized light microscopic images of calcareous nannofossil index fossil species from the early Pliocene. Note. Fossil zones assigned for each taxon follows Nannotax 3 (http://ina.tmsoc.org/Nannotax3/index.html). **a**, *Discoaster brouweri* (Sample 709C-4H-2, 20.0–21.0 cm) (NN9-NN18, CN7-CN12d); **b**, *Discoaster tamalis* (Sample 709C-4H-3, 10.0–11.0 cm) (NN14-NN16, CN10d-CN12a); **c**, *Discoaster asymmetricus* (Sample 709C-4H-3, 10.0–11.0 cm) (NN15-NN18, CN11a-CN12d); **d-1**, *Discoaster pentaradiatus* (Sample 709C-4H-3, 10.0–11.0 cm) (NN10-NN17, CN8-CN12b); **d-2**, Focus stacking images of the d-1 specimen; **e**, *Discoaster quadramus* (Sample 709C-4H-5, 10.0–11.0 cm) (NN10-NN17, CN8-CN12b); **f-1**, *Discoaster surculus* (Sample 709C-4H-5, 10.0–11.0 cm) (NN11a-NN17, CN9a-CN12b); **f-2**, Focus stacking images of the f-1 specimen; **g**, *Discoaster triradiatus* (Sample 709C-4H-4, 5.0–6.0 cm) (NN9-NN18, CN7a-CN12d); **h**, *Reticulofenestra pseudoumbilicus* (Sample 709C-4H-2, 20.0–21.0 cm) (NN4-NN15, CN3-CN11b); **i**, *Ceratolithus cristatus* (Sample 709C-5H-4, 5.0–6.0 cm) (NN13, CN10c- extant); **j-1** and **j-2**, *Sphenolithus abies* (Sample 709C-4H-4, 5.0–6.0 cm) (NN7-NN15, CN5b-CN11b).

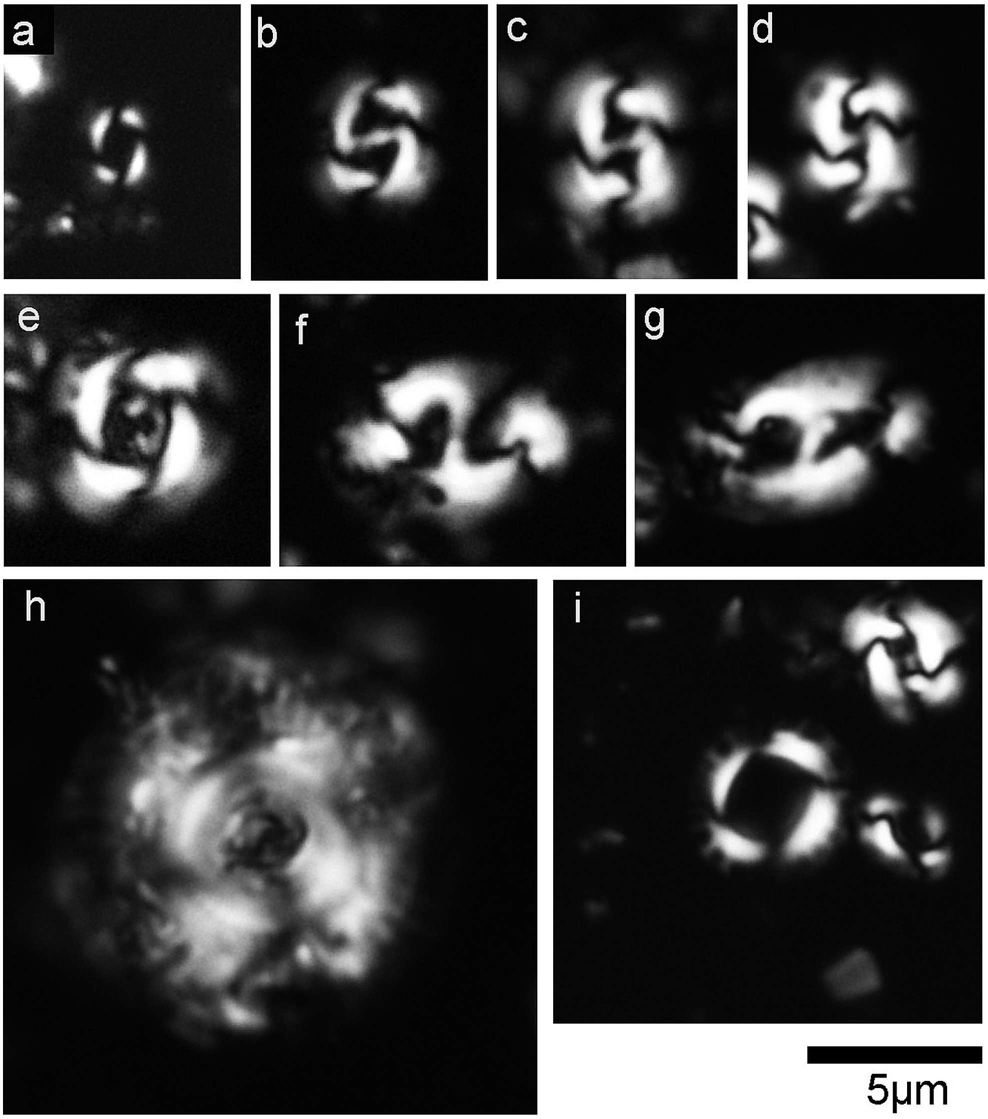

Fig. 5. Cross-polarized light microscopic images of calcareous nannofossil index fossil species from Quaternary. Note. Fossil zones assigned for each taxon follows Nannotax 3 (http://ina.tmsoc.org/Nannotax3/index.html). **a**, *Emiliania huxleyi* (Sample 709C-1H-1, 2.0–3.0 cm) (NN21-extant); **b**, *Gephyrocapsa oceanica* (Sample 709C-1H-3, 2.0–3.0 cm) (NN19-extant, CN14a-present); **c**, Large *Gephyrocapsa oceanica* (Sample 709C-2H-5, 2.0–3.0 cm) (1.46–1.24 Ma, Raffi *et al.* 2006); **d**, *Gephyrocapsa caribbeanica* (Sample 709C-2H-7, 5.0–6.0 cm) (MIS-6 to within Quaternary); **e**, *Reticulofenestra asanoi* (Sample 709C-2H-3, 2.0–3.0 cm) (NN19, CN13-CN14); **f**, *Helicosphaera inversa (*Hole 709C-1H-3, 2.0–3.0 cm) (MIS19-MIS5, Maiorano *et al.* 2013); **i**, *Pseudoemiliania lacunosa* (Hole 709C-2H-1, 2.0–3.0 cm) (NN15-NN19, CN11a-CN14a); **h**, *Calcidiscus macintyrei* (Sample 709C-3H-1, 5.0–6.0 cm) (NN17-NN19, CN12c-CN13b); **g**, *Helicosphaera sellii* (Hole 709C-3H-2, 10.0–11.0 cm) (NN12-NN19, CN10-CN14a).

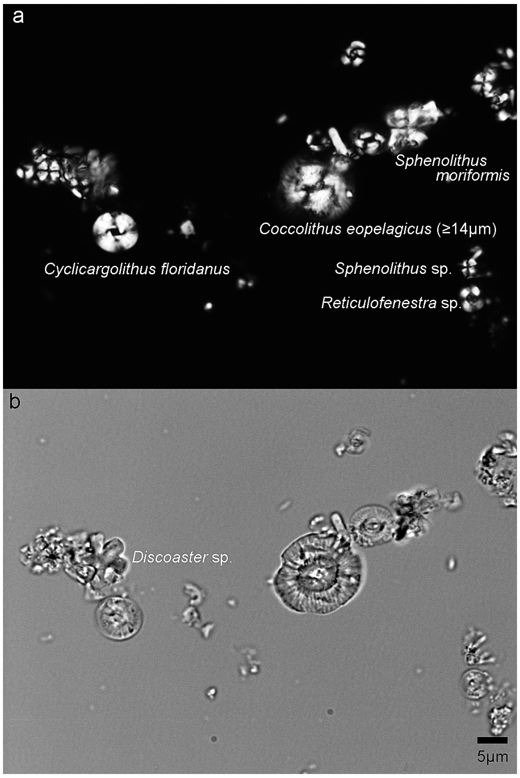

Fig. 6. Example of calcareous nannofossil assemblage in the early Miocene (Sample 709C-22X-1, 43.0–44.0 cm). **a**, Cross-polarized light microscopic image; **b**, plane-polarized light microscopic image. Note. Cross- and plane-polarized light microscopic images show an identical field of view.

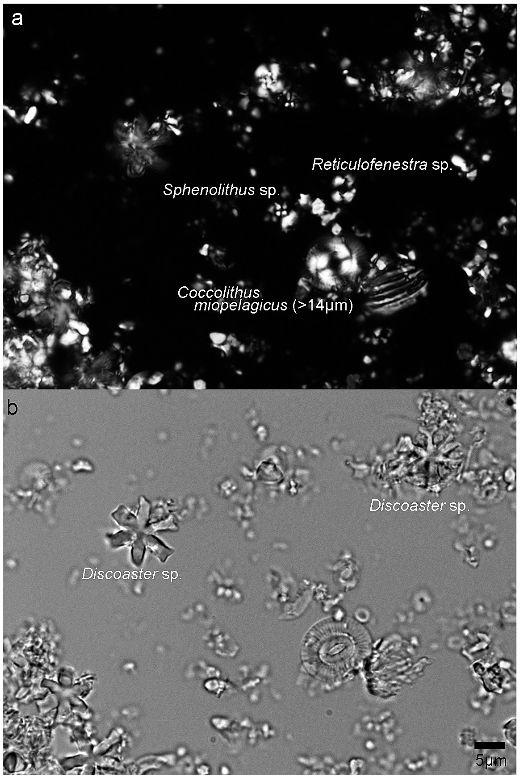

Fig. 7. Example of calcareous nannofossil assemblage in the middle Miocene (Sample 709C-13H-7, 43.0–44.0 cm). **a**, Cross-polarized light microscopic image; **b**, plane-polarized light microscopic image. Note. Cross- and plane-polarized light microscopic images show an identical field of view.

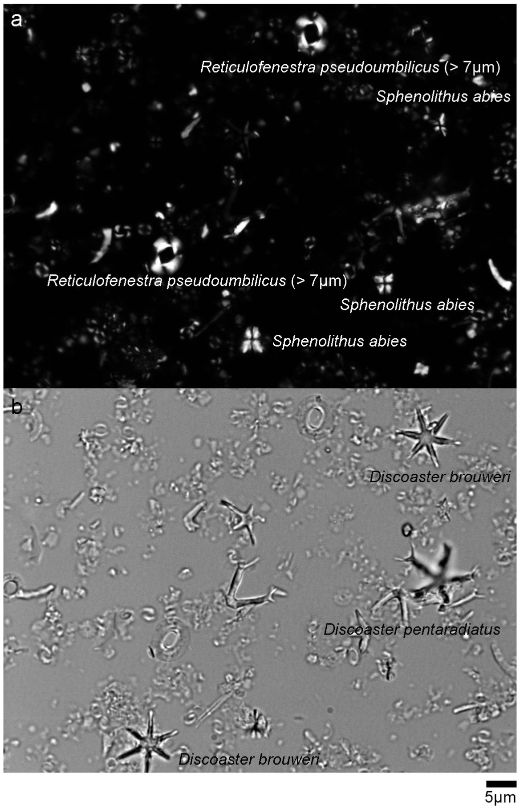

Fig. 8. Example of calcareous nannofossil assemblage from the early Pliocene (Hole 709C-5H-5, 10.0–11.0 cm). **a**, Cross-polarized light microscopic image; **b**, plane-polarized light microscopic image. Note. Cross- and plane-polarized light microscopic images show an identical field of view.

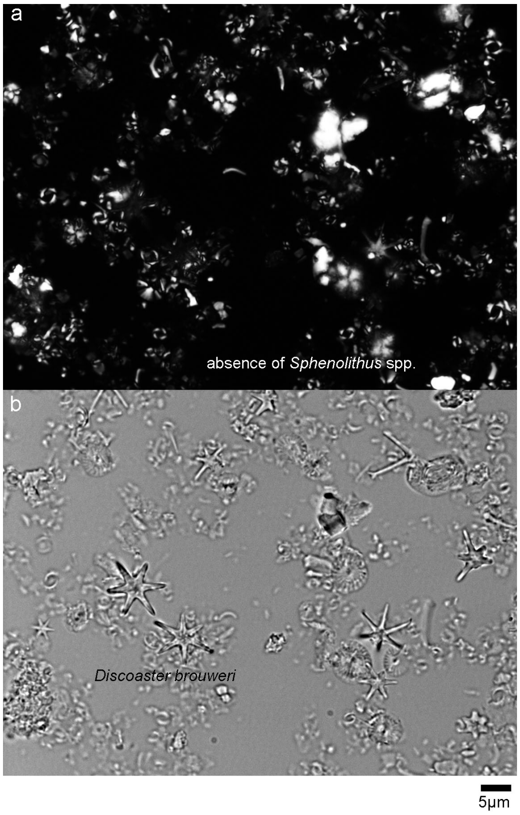

Fig. 9. Example of calcareous nannofossil assemblage in the early Pleistocene (Sample 709C-4H-1, 2.0–3.0 cm). **a**, Cross-polarized light microscopic image; **b**, plane-polarized light microscopic image. Note. Cross- and plane-polarized light microscopic images show an identical field of view.

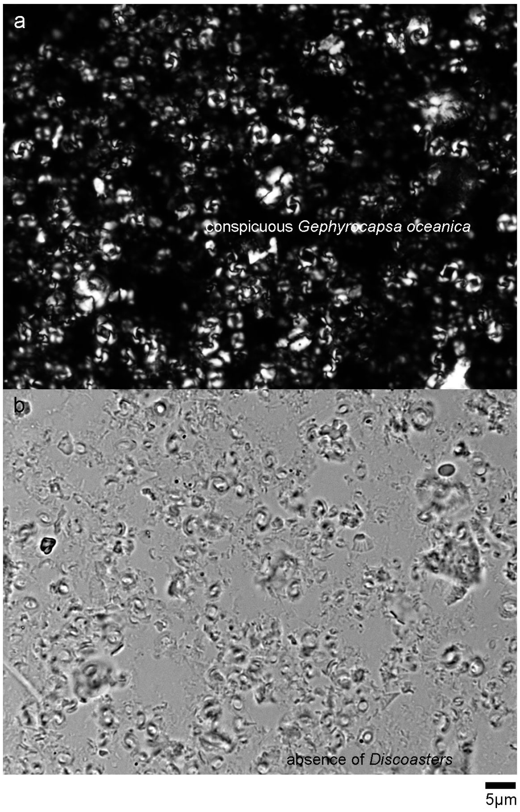

Fig. 10. Example of calcareous nannofossil assemblage in the Pleistocene younger than 1.73 Ma (Sample 709C-2H-1, 2.0–3.0 cm). **a**, Cross-polarized light microscopic image; **b**, plane-polarized light microscopic image. Note. Cross- and plane-polarized light microscopic images show an identical field of view.

eous nannofossil assemblages from 3.6–1.95 Ma (NN16-18 in Martini, 1981; CN12a-12d in Okada and Bukry, 1980) are characterized by diverse *Discoaster* spp. with Late Pliocene forms (Figs. 4a–4 g) and small–medium sized specimens of *Reticulofenestra* spp. Sediments of this age interval lack *Sphenolithus* spp. and *R. pseudoumbilicus* (≥ 7 μm) (Fig. 9) In this age interval, members of *Discoaster* (Fig. 4a–g) are useful for dating sediments (Fig. 4).

Quaternary calcareous nannofossil assemblages younger than 1.95 Ma (NN19-21 in Martini, 1971; CN13a-15 in Okada and Bukry, 1980) are characterized by dominance of the Noelaerhabdaceae (*Emiliania huxleyi*, *Gephyrocapsa* spp., and *Reticulofenestra* spp.) (Figs. 5, 10). Discoasteraceae and *Amaurolithus* spp., which are invisible/obscure under cross-polarized light, are absent in this age interval (Fig. 10), and all biostratigraphically significant calcareous nannofossil taxa which occur from 1.9 Ma to the present are visible in the cross-polarized light. In sediments younger than 1.95 Ma, occurrence of large *Gephyrocapsa* (>5.5 μm) (ca. 1.6–1.2 Ma) (Fig. 5c), *Reticulofenestra asanoi* (>6.5 μm) (ca. 1.1–0.9 Ma) (Fig. 6e), and disappearance of *Calcidiscus macintyrei* (*Calcidiscus* with central opening larger than 11 μm) (1.1 Ma) (Fig. 5h) can be used for dating of sediments together with other index species (Raffi *et al.*, 2006).

Concluding Remarks

In this study, we have prepared reference smear slides for calcareous nannofossil learners from Miocene to Pleistocene sediments, these slide sets are documented here and we briefly introduced major index species and change in calcareous nannofossil assemblages in the period. For more practical study of calcareous nannofossil biostratigraphy, understanding of various calcareous nannofossil taxa is necessary. Miocene–Pleistocene calcareous nannofossil biostratigraphy and the occurrence record of each taxon are summarized in various papers, notably including Backman *et al.* (2012), Hine and Weaver (1998), Perch-Nielsen (1985), Raffi *et al.* (2006), and Young (1997). In addition the website Nannotax 3 (http://ina.tmsoc.org/Nannotax3/index.html) is useful for self-education of Miocene-Pleistocene biostratigraphy.

Acknowledgements

We thank Hisatake Okada for his suggestion on this manuscript. Samples used for this study were provided by the Ocean Drilling Program (021685-IODP). We acknowledge Dr. Young of the UCL for his critical review. This study was supported by Grant-in-aid for Scientific Research from the Japan Society for the Promotion of Sciences (No. 26400505).

Reference

Backman, J., Raffi, I., Rio, D., Fornaciari, E. and Pälike, H. (2012). Biozonation and biochronology of Miocene through Pleistocene calcareous nannofossils from low and middle latitudes. *Newsletters on Stratigraphy*, **45**: 221–244.

Bown, P. R. (1998). Calcareous Nannofossil Biostratigraphy. 315 pp. Kluwer Academic Publishers, London.

Hine, N. and Weaver, P. P. E. (1998). Quaternary. In: Bown, P. R. (Ed.), Calcareous Nannofossil Biostratigraphy. Chapman & Hall, London, pp. 266–283.

Maiorano, P., Tarantino, F., Marino, M. and Girone, A. (2013). A paleoecological and paleobiogeographic evaluation of Helicosphaera inversa (Gartner) Theodoridis and the diachrony of its First Occurrence. *Marine Micropaleontology*, **104**: 14–24.

Martini, E. (1971). Standard tertiary and quaternary calcareous nannoplankton zonation. In: Farinacci, A. (Ed.), Proceedings of the 2nd Plankton Conference, Rome, 1970, pp. 737–785.

Okada, H. (1990). Quaternary and Paleogene Calcareous Nannofossils. *Proceedings of the Ocean Drilling Program*, *Scientific Results*, **115**: 129–174.

Okada, H. and Bukry, D. (1980). Supplementary modification and Introduction of code numbers to the low-latitude coccolith biostratigraphy zonation (Bukry, 1973; 1975). *Marine Micropaleontology*, **5**: 321–325.

Raffi, I., Backman, J., Fornaciari, E., Palike, H., Rio, D., Lourens, L. J. and Hilgen, F. J. (2006). A review of calcareous nannofossil astrobiochronology encompassing the past 25 million years. *Quaternary Science Reviews*, **25**: 3113–3137.

Rio, D., Fornaciari, E. and Raffi, I. (1990). Late Oligocene through early Pleistocene calcareous nannofossils from western equatorial Indian Ocean (Leg 115). *Proceedings of the Ocean Drilling Program*, *Scientific Results*, **115**: 175–235.

Shipboard Scientific Party (1988). Site 709. In: Backman, J., Duncan, R. A. *et al.* (Eds.), Proceedings of the Ocean Drilling Program, Initial Reports, College Station, TX, pp. 459–588.

Young, J. R. (1998). Neogene. In: Bown, P. R. (Ed.), Calcareous Nannofossil Biostratigraphy. Chapman & Hall, London, pp. 225–265.